Simulation studies of the fidelity of biomolecular structure ensemble recreation

3 **AUTHORS**, INCLUDING:

Peter Wolynes
Rice University

359 PUBLICATIONS **29,029** CITATIONS

Simulation studies of the fidelity of biomolecular structure ensemble recreation

Joachim Lätzer[a)]
Department of Chemistry and Biochemistry, University of California, San Diego, La Jolla, California 92093-0365 and NSF Center for Theoretical Biological Physics (CTBP), University of California, San Diego, La Jolla, California 92093-0365

Michael P. Eastwood[b)]
Department of Chemistry and Biochemistry, University of California, San Diego, La Jolla, California 92093-0365

Peter G. Wolynes[c)]
Department of Chemistry and Biochemistry, University of California, San Diego, La Jolla, California 92093-0365 and NSF Center for Theoretical Biological Physics (CTBP), University of California, San Diego, La Jolla, California 92093-0365

We examine the ability of Bayesian methods to recreate structural ensembles for partially folded molecules from averaged data. Specifically we test the ability of various algorithms to recreate different transition state ensembles for folding proteins using a multiple replica simulation algorithm using input from "gold standard" reference ensembles that were first generated with a Gō-like Hamiltonian having nonpairwise additive terms. A set of low resolution data, which function as the "experimental" ϕ values, were first constructed from this reference ensemble. The resulting ϕ values were then treated as one would treat laboratory experimental data and were used as input in the replica reconstruction algorithm. The resulting ensembles of structures obtained by the replica algorithm were compared to the gold standard reference ensemble, from which those "data" were, in fact, obtained. It is found that for a unimodal transition state ensemble with a low barrier, the multiple replica algorithm does recreate the reference ensemble fairly successfully when no experimental error is assumed. The Kolmogorov-Smirnov test as well as principal component analysis show that the overlap of the recovered and reference ensembles is significantly enhanced when multiple replicas are used. Reduction of the multiple replica ensembles by clustering successfully yields subensembles with close similarity to the reference ensembles. On the other hand, for a high barrier transition state with two distinct transition state ensembles, the single replica algorithm only samples a few structures of one of the reference ensemble basins. This is due to the fact that the ϕ values are intrinsically ensemble averaged quantities. The replica algorithm with multiple copies does sample both reference ensemble basins. In contrast to the single replica case, the multiple replicas are constrained to reproduce the average ϕ values, but allow fluctuations in ϕ for each individual copy. These fluctuations facilitate a more faithful sampling of the reference ensemble basins. Finally, we test how robustly the reconstruction algorithm can function by introducing errors in ϕ comparable in magnitude to those suggested by some authors. In this circumstance we observe that the chances of ensemble recovery with the replica algorithm are poor using a single replica, but are improved when multiple copies are used. A multimodal transition state ensemble, however, turns out to be more sensitive to large errors in ϕ (if appropriately gauged) and attempts at successful recreation of the reference ensemble with simple replica algorithms can fall short. © *2006 American Institute of Physics.* [DOI: 10.1063/1.2375121]

I. INTRODUCTION

The most studied proteins in the cell fold to a reasonably well-defined, average native conformation. The fact that folding times of proteins are relatively short when compared to the time needed for the protein chain to explore all its possible conformations leads to the conclusion that the pro-

tein must be guided towards the native state. The contacts formed in this native conformation must on average be more stabilizing than random contacts allowing the protein molecule to fold to the native conformation by trading entropy for energy. This principle of minimal frustration[1] captures the essential physics of the folding of naturally evolved proteins. The energy landscape of protein folding for proteins that fold reliably therefore resembles a rough funnel.[2] Energy landscape theory describes the folding process down the funnel as a progressive organization of ensembles of partially

---

a)Electronic mail: jlatzer@ucsd.edu
b)Present address: D. E. Shaw Research, LLC, New York, New York 10036.
c)Electronic mail: pwolynes@ucsd.edu

folded structures.[3] For two-state folders owing to uneven compensation of entropy loss by stability gain, there is a bottleneck in the flow between the folded and unfolded minima in the free energy which represents the transition state. In the energy landscape ensemble view, the transition state is best described as an ensemble of configurations rather than a single structure.[4]

Many experimental techniques have been developed to infer structural information about the structural ensembles for incompletely structured proteins along the folding funnel. With the exception of single molecule studies, those experiments that do provide structural information along the folding funnel typically provide only ensemble averaged quantities. For long lived intermediates, these measured averages directly include NMR parameters and fluorescence resonance energy transfer (FRET) distances, and sometimes structural averages can indirectly be inferred through H/D exchange profiles which are, however, intrinsically kinetic. Using the assumption of a funneled landscape, similar information can often be obtained for the fleeting transition state. The protein-engineering method[5] developed by Matouschek et al. provides (for smooth landscapes) structural information about the transition state ensemble analogous in many respects to NMR data obtained for long-lived intermediates. This approach assigns a ϕ_i^{expt} value to each residue. The ϕ_i^{expt} value is defined as the ratio of the change of the apparent free energy difference between the transition state ensemble and unfolded state ensemble upon a conservative mutation of the residue i to the change in free energy between the native and unfolded ensembles free energy with the same mutation. A ϕ_i^{expt} value of unity for a residue would indicate that the changes in free energy made by this residue in the transition state are the same as the changes in the native state, whereas a ϕ_i^{expt} value of zero would indicate that this residue has no nativelike interactions. Assuming that the native contacts in the protein alone account for the stabilizing interactions,[6] a ϕ_i^{expt} value can then be approximated as the fraction of native contacts made[7] and this averaged structural quantity can be used as a restraint in molecular dynamics simulations.[8–12] Technically, this identification is only valid for a perfectly homogeneous funnel landscape. Defining a contact distance R_C for interacting amino acids, the determined ϕ values can then be used as constraints on the ensemble of protein structures, requiring each residue to form a fraction of its native contacts to within an upper distance bound R_C. The measured constraints, however, do not enforce a precise distance for two residues in contact. This raises the question whether (or when) ensembles deduced from the ϕ-value constraints are structurally equivalent to the actual ensemble probed by the experiment. That is, can the real ensemble be faithfully recreated from experimental data alone? Also do some algorithms give greater fidelity in reconstruction than do others? In particular, the experimentally derived restraints may be applied equally to every structure encountered on a single molecular dynamics (MD) trajectory (the "single replica" case); alternatively a multiple replica algorithm may be used where the restraints are applied to the ensemble of structures observed in a number of simultaneous MD simulations

thereby allowing individual replicas to have fluctuations while restraining the ensemble average. Davis et al.[13] have already shown that in the case of the β3s peptide two replicas were required to correctly predict the transition state structures from the ensemble-average set of ϕ values. This result encourages examining more quantitatively the benefits of using multiple replica algorithms.

Here we present an extension of the multiple replica approach to the simultaneous determination of a transition state ensembles. We test this approach by attempting the recreation of a completely known, candidate transition state ensemble of 500 structures of the λ-repressor protein. First we create several surrogates for the "experimental transition state ensembles," which we shall term reference ensembles, sampled from simulations using native structure based[14] Hamiltonians for the λ repressor both with and without nonpairwise-additive interaction terms. From the reference ensembles we calculate the average ϕ value for each residue. These computed ϕ values then serve as surrogate experimental constraints for the replica simulation algorithm. Single and multiple replica molecular dynamics simulations are then performed with a Hamiltonian that biases the ensembles to match the experimental ϕ-value constraints but otherwise has no a priori biases. Since the structures of the reference ensembles are known, the success of recreating the original ensemble using the multiple replica algorithm can be rigorously evaluated with a statistical test, the Kolmogorov-Smirnov test.[15] In the Kolmogorov-Smirnov (KS) test two ensemble distributions, one given by the reference ensembles and the other given by the ensembles obtained in the replica molecular dynamics simulations, are compared and it is tested whether these two distributions are substantially the same. When the two ensembles differ, a method can be used to uncover possible matching subensembles from the ensembles obtained in the replica molecular dynamics simulations. These subensembles can be obtained by clustering the structures and selecting the most dominant cluster as a representative ensemble. These representative subensembles can then also be compared to the reference ensembles. To study whether multiple replica recreation methods are more faithful than single copy approaches, we first analyze the principal components of the contact maps of all structures in the reference ensembles and in the ensembles obtained in the replica simulations. The principal component analysis indicates that the sampling is improved, when multiple replicas are introduced. Finally we probe the robustness of the ensemble recovery to realistic uncertainty in the input data. Experimental quantities always have errors associated with them. To mimic these errors, we assigned new ϕ values for each residue by generating a random number drawn from a Gaussian distribution with its maximum located at the original ϕ value of that residue and with a variance given by the variance of that ϕ value in the reference ensemble. The new set of ϕ values then served as input for the replica Hamiltonian ensemble reconstruction. The ensembles obtained from the replica algorithm with the new set of ϕ values as experimental constraints were compared to the original

reference ensemble. This procedure quantitatively probes how large errors in ϕ can substantially reduce the chances of faithful ensemble recreation using replica simulation algorithms.

II. METHODS

A. Reference ensemble creation

In order to rigorously test the fidelity of a reconstruction procedure a well characterized reference ensemble must first be available. An off-lattice simulation with a native structure based Hamiltonian[16] with variable strength nonadditive terms as described in detail earlier[14] was chosen to provide such reference ensembles for the reconstruction procedure. These reference ensembles are considered "gold standard" ensembles and represent the ensembles that experiments strive to determine. The energy function used to obtain these ensembles is given as the sum of a native structured based but nonadditive Hamiltonian H_{na} and standard backbone energy terms,

$$H = H_{backbone} + H_{na}. \qquad (1)$$

This energy function applies to a reduced set of coordinates of the heavy backbone atoms, C^α, C^β, and O. In this reduced description, the positions of the nitrogen and C' carbons can be calculated assuming ideal protein backbone geometry. The backbone potential takes on the following form:

$$H_{backbone} = \lambda_{\psi\phi}V_{\psi\phi} + \lambda_\chi V_\chi + \lambda_{ex}V_{ex} + \lambda_{harm}V_{harm}. \qquad (2)$$

The backbone terms[17] in the Hamiltonian ensure that the backbone has physically allowable conformations. The planarity of the peptide bond is constrained by the SHAKE algorithm and three simple harmonic potentials V_{harm}, which restrain the nitrogen-C^β, nitrogen-C', and C'-C^β distances close to 2.46, 2.45, and 2.51 Å, respectively. A chirality potential V_χ biases the C^α atoms towards the L configuration which is preferred in nature. The ϕ and ψ angles of the protein backbone are biased with the Ramachandran potential $V_{\psi\phi}$. This potential biases the torsional angles of the protein to regions allowable for a naturally occurring protein. The barriers between minima of the Ramachandran potential are intentionally set low to facilitate more rapid chain dynamics. Excluded volume effects are included between C^α-C^α, C^α-C^β, C^β-C^β, and O–O pairs through the V_{ex} potential. The individual λ parameters in the backbone Hamiltonian scale the interactions to physically reasonable values.

The H_{na} energy depends on Gaussian interaction terms for native contact pairs only. H_{na} is given as a function of pairwise energy terms raised to the power p.

$$H_{na} = -\frac{1}{2}\sum_i |E_i|^p. \qquad (3)$$

The parameter p in the Hamiltonian is the power of nonadditivity and introduces $(p+1)$-body interactions as well as p, $p-1, \ldots, 2$-body interactions with range $r_C = 8.0$ Å. Usually increasing p results in additional cooperativity and hence in increased barrier heights for folding. The individual pairwise energy terms can be written in a normalized form containing a cutoff distance r_c.

$$E_i = \sum_j \epsilon_{ij}(r_{ij}) = -\sum_j \left|\frac{\epsilon}{a}\right|^{1/p} \theta(r_c - r_{ij}^N) \gamma_{ij}$$
$$\times \exp\left(-\frac{(r_{ij} - r_{ij}^N)^2}{2\sigma_{ij}^2}\right). \qquad (4)$$

The contribution of H_{na} to the native state energy of a protein with N residues is by definition $4N\epsilon$. This is ensured if the normalization constant a is defined as

$$a = \frac{1}{8N}\sum_i \left|\sum_j \gamma_{ij}\theta(r_c - r_{ij}^N)\right|^p. \qquad (5)$$

The weighting function γ and the well width σ depend on the sequence separation of residues i and j and are chosen such that the energy of the ground-state energy for $p=1$ at a cutoff distance of $r_c = 8$ Å is evenly divided between short ($|i-j| < 5$) and long range interactions in sequence space as suggested by the analysis of Saven and Wolynes for helical proteins.[18] The parameters are

$$\sigma_{ij} = |i-j|^{0.15} \text{ Å},$$

$$\gamma_{ij} = \begin{cases} 0.125 & |i-j| < 5 \\ 0.5 & \text{otherwise}. \end{cases} \qquad (6)$$

The total Hamiltonian described above can be used to infer the thermodynamic properties of a given system. To obtain useful free energy profiles, a proper reaction coordinate has to be chosen. One appropriate coordinate is Q, a measure of native likeness,

$$Q = \frac{2}{(N-1)(N-2)}\sum_{i<j-1} \exp\left(-\frac{(r_{ij} - r_{ij}^N)^2}{2\sigma_{ij}^2}\right), \qquad (7)$$

Q is a normalized quantity that describes structural similarity of a given structure with coordinate set $\{r_{ij}\}$ to a reference structure, for folding and structure prediction usually the native structure, with coordinates $\{r_{ij}^N\}$. Free energy profiles were then obtained with the weighted histogram analysis method (WHAM) with umbrella sampling. 17 constant temperature molecular dynamics simulations were performed with a biasing potential that is a polynomial in Q of fourth order centered on different values of Q ($Q_0 = 0.9$, 0.85, 0.8, 0.1) to obtain good phase-space sampling along this reaction coordinate. The Q constraint in the potential is sequentially reduced from $Q=0.9$, which is almost nativelike, to $Q=0.1$. This procedure reduces the equilibration time of the system. During each of these constant temperature molecular dynamics simulation, 200 independent samples N_s^{obs} of Q and energy E, the backbone and H_{na} energy, were collected at regularly spaced time steps. These time steps were larger than the correlation time between sampled structures. The samples therby obtained were independent of earlier configurations sampled. The first 40 samples of each simulation run were discarded to help ensure that the system reached equilibrium, before samples were entered into the free energy calculation. A histogram $N_s(E, Q)$ for all 17 simulations was created. The

density of states $n(E,Q)$ of the system (Eastwood et al., 2001) was calculated from the histograms

$$n(E,Q) = \sum_s w_s(E,Q) \frac{N_s(E,Q)}{N_s^{\text{obs}}} Z_s(\beta_s) \exp(\beta_s(V_s(Q)+E)).$$

(8)

Here s labels the simulation and w represents a weighting function defined as

$$w_i = \frac{A_s^{-2}}{\sum_m A_m^{-2}},$$

(9)

$$A_s^{-2} = \frac{n(E,Q)}{N_s^{\text{obs}}} Z_s(\beta_s) \exp(\beta_s(V_s(Q)+E)).$$

The density of states and the weighting function are functions of the partition function Z_s. The partition function, on the other hand, is also a function of the density of states,

$$Z_s(\beta_s) = \sum_{E,Q} n(E,Q) \exp(-\beta_s(V_s(Q)+E)).$$

(10)

This set of equations can be used to obtain for $n(E,Q)$ self-consistently to within a multiplicative constant and hence the free energy was obtained to within a constant as

$$F(Q,T) = -k_B T \log\left(\sum_{E,Q} n(E,Q) \exp\left(-\frac{E}{k_B T}\right)\right).$$

(11)

The free energy profile at folding temperature T_f can be inspected and ensembles for the denatured state, the transition state, or any other reference state of choice can be found by Q. Structures with the appropriate Q value entered into the reference ensemble.

B. ϕ-value molecular dynamics replica simulation technique and details

Given a set of experimental ϕ values $\{\langle\phi_i\rangle_{\text{exp}}\}$ for the residues of the protein, we can write down a replica Hamiltonian that constrains ensemble averages to the values provided by experimental measurements for each residue. The simplest form of the replica Hamiltonian contains standard backbone terms as described above while adding the experimental biasing potential. Optionally other energy terms, H_{funnel}, that vary the protein energy landscape and encode prior theoretical expectations can also be included. In this paper H_{funnel} will be set to 0.

$$H_{\text{rep}} = H_{\text{back}} + H_{\text{funnel}} + \sum_{i=1}^N \lambda_i(\overline{\phi_i} - \langle\phi_i\rangle_{\text{expt}})^2,$$

(12)

with N being the total number of residues. The ensemble average ϕ value $\overline{\phi_i}$ is the arithmetic average over the realizations of the individual replicas.

$$\overline{\phi_i} = \frac{1}{N_{\text{rep}}} \sum_{\mu=1}^{N_{\text{rep}}} \phi_i^\mu,$$

(13)

where N_{rep} is the number of simulated replicas. To perform molecular dynamics simulations, a recipe to calculate ϕ from the observed contacts must be given. Although ϕ is a dynamical quantity measured from the ratio of thermodynamic and kinetic quantities, an often used surrogate for ϕ is the ratio of native contacts made divided by the maximum number of native contacts possible. This surrogate, of course, assumes the landscape is, in fact, reasonably funneled.[19] An explicit equation for ϕ_i^μ in terms of a contact function c_{ij} is

$$\phi_i^\mu = \frac{1}{N_{\text{cont}}^i} \sum_{\langle j\rangle} c_{ij} = \frac{1}{N_{\text{cont}}^i} \sum_{\langle j\rangle} \frac{1}{2}(1 + \tanh(5(r_c - r_{ij}))) \quad (14)$$

The contact function considers native contacts to be formed only if they reside within some cutoff distance r_c. The cutoff distance for C^β contacts usually lies in the region of 6.5–8.5 Å. In the present study cutoff distances of 6.5 and 8.0 Å have been used. We only present results for a cutoff distance of 6.5 Å. The definition of the set of contacts for the completely native structure depends on the value of the cutoff distance between the C^β's. Once a value for the cutoff distance is chosen, the appropriateness of this value for defining contacts can be checked for consistency with other methods of assigning contacts such as the CSU algorithm which rely on all-atom structural information. The functional form of the contact function is a tanh function, whose continuous nature prevents numerical errors in the dynamics.

The simulation scheme used is as follows: Constant temperature molecular dynamics simulations are performed at three temperatures, T_F $0.25T_F$, and $1.75T_F$ for 1, 2, 4, and 8 replicas. The folding temperature T_F corresponds to the "physiological" transition temperature for folding of the nonadditive Gō-like energy function described above. The simplicity of the model allows extensive sampling to be done. It is straightforward to employ simulations of length of the order of 1 ms. This time scale ensures enough sampling to compensate for topological traps in the energy landscapes. The results are checked to ensure they converged. The simulations involve different numbers of replicas, but the total number of sampled conformations is kept constant between simulation runs with different numbers of replicas. The ensembles can now be fairly compared.

We first test to make sure that the input ϕ values are reproduced. Next a statistical test is used to decide whether ensembles generated from the replica algorithm differ from the reference ensemble or not. An appropriate statistical test for comparing ensemble distributions is the the KS test. The KS test quantifies whether two distributions differ from each other in a statistically significant way. To apply the KS test, the ensembles are first reduced to distributions that are functions of only a single, independent variable. This single independent variable is chosen to be a structural overlap measure q defined analogously to Q, but where all q's of the structures in the ensemble are measured relative to each other rather than measured to one single reference structure. The KS test requires calculation of distributions of q for all pairs of structures within the simulated ensemble ($P_B(q)$), all pairs within the reference ensemble ($P_A(q)$), and all pairs with one member chosen from each of the two ensembles ($P_{AB}(q)$). The KS test is then performed on the individual distributions, which tests if two distribution are statistically

identical, typically we compare $P_A(q)$ with $P_{AB}(q)$. In our case where we have a large amount of data when comparing two different Hamiltonians, the result of the test indicate that the two distributions are not exactly the same. However, the KS statistics itself provides a very useful measure for quantifying the magnitude of the difference, and simply visualizing the difference between the distributions is illuminating.

C. Principal component analysis

Contact maps for the reference ensemble and the ensembles obtained from the replica simulations were computed for all individual structures. Principal component analysis (PCA) of the binary contact degrees of freedom for these ensemble structures was performed.[20] The PCA we employ is not the more commonly used PCA based on Cartesian coordinates. The more commonly used PCA is based on the diagonalization of the Cartesian coordinates. This is less useful in the current problem due to the fact that the transition state ensembles generally show large anharmonic conformational differences that go beyond simple vibrational-like fluctuations of Cartesian coordinates. This approach uses a very coarse-grained degree of freedom: the contact map, which is the simplest site specific measure of a folding progress. To facilitate the analyses, we further coarse grained the contacts by grouping neighboring residues into groups of three residues, i.e., a coarse-grained contact matrix is calculated for each structure, with each of those independent elements either being 0 or 1. The contacts are reduced to $27 \times (27-1)/2 = 378$ elements that are either 0 or 1. The resulting reduced covariance matrix of dimension 378×378 is diagonalized and the eigenvalues for the contact map PCA are calculated. The two most dominant principal components are plotted.

D. Structural clustering analysis

The Fitch-Margoliash algorithm[21] is a distance based bioinformatic algorithm to fit a phylogenetic tree to a distance matrix. The numerous structures obtained from the simulation runs were clustered using the FITCH program of the PHYLIP package.[22] The FITCH program can be used to create phylogenetic trees based on any given distance measure. In order to analyze the structures obtained in the simulated annealing with the bioinformatic software, a topology based distance measure d between two structures A and B was defined through the structural overlap q as $d = 1 - q$. The order parameter q represents the relative similarity of two structures and is defined analogously to Q. Since q is a normalized measure of the fraction of overlapping contacts, d is a measure of how dissimilar two structures are in terms of their contacts. Similar structures with small d are close and dissimilar structures with large d are structurally far away. Since q, unlike ϕ, is sensitive to the correct distance between residues rather than just constraining two residues to be within a cutoff distance, the clustering should group all structures based on their local secondary global as well as their global tertiary structure. This clustering technique helps in extracting subensembles with more narrowly defined local structures.

III. RESULTS FOR THE TRANSITION STATE ENSEMBLE OF THE λ REPRESSOR

We first present the complete results of ensemble recovery with replicas for the transition state ensemble of the λ repressor. The λ repressor is a well studied DNA-binding regulatory protein with a four helix bundle fold. Experimental data suggest that the λ repressor is a two-state folder with a low barrier between folded and unfolded basins.[23] To test the inversion algorithm, reference ensembles for the λ repressor [protein data bank (pdb) code 1lmb (Ref. [24])] were first generated with the nonadditive Gō-like Hamiltonian using Q as a reaction coordinate. Although there has been controversy about the merits of Q as a reaction coordinate,[25] this controversy is irrelevant for our present purpose of obtaining reference transition-state ensembles which are only to be used as test beds for studying the reproduction of an ensemble from its averaged properties alone. To assure the reader of the validity of the ensembles obtained with this Hamiltonian, we note that it has already been tested whether these Hamiltonians with many-body interactions produce ensembles, that resemble ensembles one would measure in experiments. This has been done by testing the correlation of experimental ϕ values and experimental folding rates to the ϕ values and folding rates obtained with the nonadditive Hamiltonian. It has been shown that great agreement with experiment can be reached, when the fraction of energy arising from three-body terms in the native state is approximately 20%.[26] A power of nonadditivity in the range $p = 2-3$ for our Hamiltonian should lead to nonadditive contributions to the energy of a magnitude found in real proteins.[14] WHAM simulations with umbrella sampling were performed at the putative folding temperature $k_B T / \epsilon = 1.0$. The free energy profiles were then calculated as described in the Methods section. To obtain a more refined estimate of the folding temperatures the free energy profiles were extrapolated to nearby temperatures to find the temperature where the depths of the folded and unfolded basins coincide. Further WHAM simulations with umbrella sampling were then performed at this new temperature. The free energy profiles were calculated with the new data yielding a more accurate estimate of T_F. This procedure was repeated until convergence, which in practice occurred after only two rounds of WHAM simulations. The free energy profiles of the λ repressor at $T_F = 0.97$, 1.02, and 0.93 for a classical native structure based Hamiltonian with $p = 1$ and for Gō-like Hamiltonians with many-body effects for $p = 2$ and 3 respectively are shown in Fig. 1. The free energy curves exhibit a two-state folding character with a barrier between folded and unfolded states, that increases with increasing parameter p. For $p = 1$ and 2 the barrier between unfolded and folded basins is roughly $\sim 1 k_B T_F$ indicating that the weak cooperative effects present. Introduction of four body terms corresponding to $p = 3$ increases the barrier roughly tenfold to about $\sim 8 k_B T_F$. Various reference ensembles are then read off the free energy profile. The Q score of the transition state ensemble was determined at the maximum value of the free energy curve between the folded and unfolded basins. The transition state ensembles had a Q score of about $Q = 0.5$. Approximately 500 independently sampled structures were chosen for each
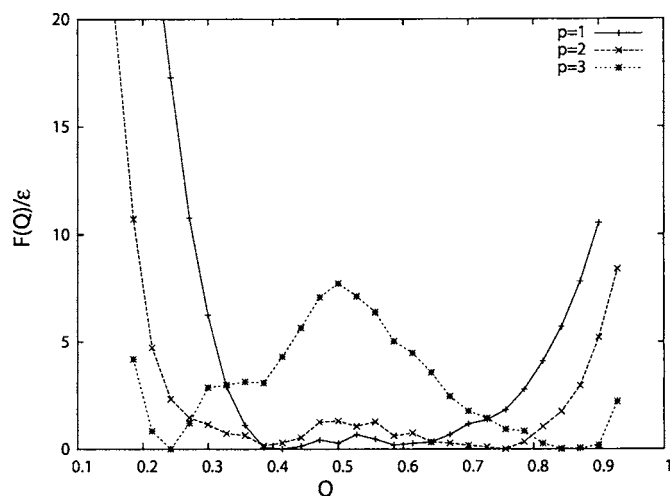
FIG. 1. Free energy profiles at folding temperature T_F as a function of Q obtained with WHAM and umbrella sampling with the nonadditive Hamiltonian. The free energy shows two-state behavior with increasing barrier for increasing p, the power of nonadditivity. The free energy profile shows a transition state ensemble at $Q \approx 0.5$.

transition state ensemble for $p=1$, 2, and 3 to represent the reference ensemble. The contact maps for the ensembles obtained with $p=1$ and $p=3$ are shown in Fig. 2. Contact maps of native contacts only are shown above the diagonal whereas both native and non-native contacts are shown below the diagonal. From the native contact maps it is apparent that the C-terminal and the long N-terminal helix are most ordered in the transition state ensemble. The DNA binding site (pdb residues 34–54) is most disordered in the transition state. The reference ensembles also show several non-native contacts with low contact probability in the ensemble.

The inversion algorithm derives structures only from the input ϕ values, which are calculated from native contacts. The ϕ value is defined as a fraction of native contacts, where contacts are defined to fall within a certain cutoff distance. The inversion of such data might then be not accurate on the more local level due to the lack of secondary structure information in the inversion Hamiltonian and lack of knowledge of low-probability non-native contacts. A set of ϕ values denoted $\{\langle\phi_i\rangle_{\mathrm{expt}}\}$ and the corresponding (in this case, statistical) error $\delta\phi_i$ was calculated for each of the reference ensembles. The native structure of the protein, the $\{\langle\phi_i\rangle_{\mathrm{expt}}\}$, and (in some cases) the statistical errors were the only data used to infer the transition state ensembles. The simplest energy function, that can be used to recover ensembles from the given information, is a Hamiltonian which reproduces the given ensemble averaged constraints but that has no knowledge of the energy landscape of folding of the protein. Such a basic Hamiltonian is given in Eq. (12) with $H_{\mathrm{funnel}}=0$. The only unknown parameter in the Hamiltonian is the strength of interaction of the experimental restraint, the parameter λ. To approximately determine the parameter λ, successive ϕ-value simulations with gradually increasing values of λ were performed to set a uniform λ value for all residues such that the experimental constraints are fulfilled. Comparison of the experimental ϕ values to the simulation ϕ values showed a consistent match with high correlation for different num-
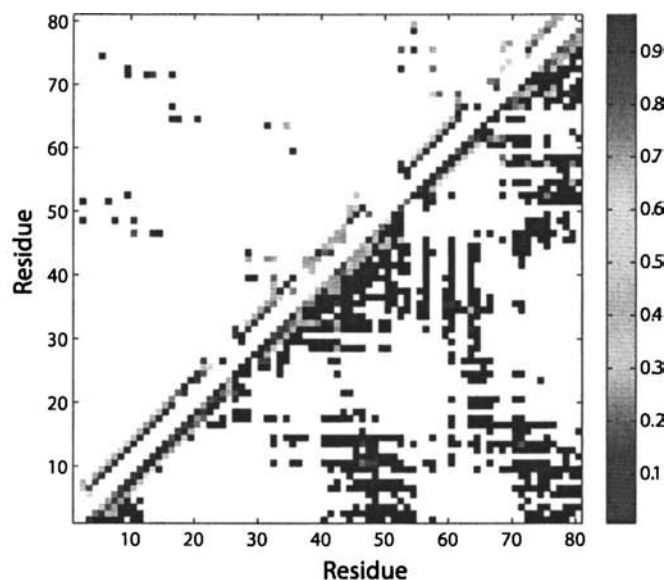
(a)
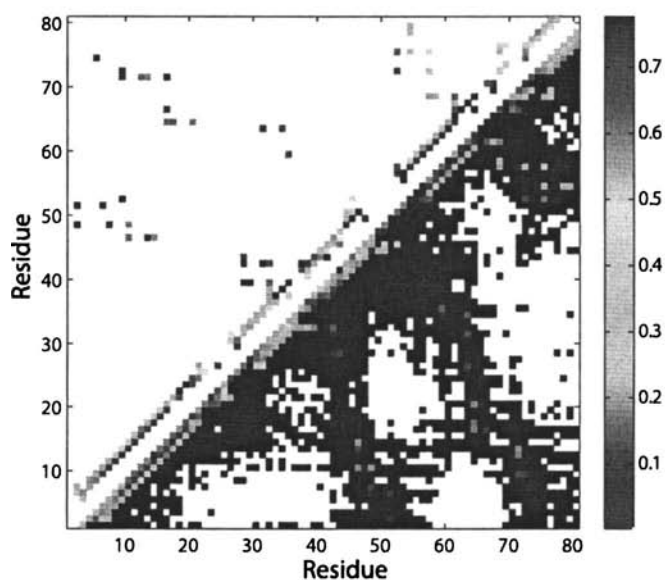
(b)

FIG. 2. Native contact map only (above diagonal) and complete contact map (below diagonal) of the transition state reference ensembles of the λ repressor for $p=1$ (a) and $p=3$ (b) averaged over all structures. A contact is defined when the distance of the C_β carbons are within 6.5 Å. A dark red contact corresponds to a contact that is on always formed in the transition state ensemble. A dark blue contact, on the other hand, is never formed in the transition state ensemble.

bers of replicas (data not shown). This indicates that the restraints in the simulation are strong enough that ensembles with the correct ϕ values for each residue are indeed produced. We note that the results for $p=2$ are very similar to those found for the $p=1$ case and discussion of the $p=2$ results will therefore be omitted. The individual ensembles obtained from the replica simulations each consisted of 1600 independently sampled structures taken from millisecond long molecular dynamics trajectories. From the structures found in the simulations with replicas and the reference ensembles probability distributions of the single independent variable q, the structural overlap reaction coordinate may be extracted. A statistical test can be performed to check

whether the ensembles obtained from the ϕ-value molecular dynamics replica simulations for one to eight replicas can be considered apart from incomplete sampling identical to the reference ensemble which was used to generate the input ϕ values. Figure 3 shows the results of the KS test for the various transition state ensembles. Two structural ensembles are equal (or there is an absence of evidence that they differ) if the probability distribution of pairwise overlaps, $P(q)$, is the same irrespective of whether the pairs are drawn from the same ensemble or from distinct ensembles. For the $p=1$ and $p=3$ transition state ensembles, the probability distribution of overlaps between the one replica and reference ensemble has some overlap with the distribution of overlaps within the reference ensemble. However, this overlap between distributions is not large, showing that the reference ensemble and the ensemble obtained from the one-replica simulation are in fact cannot be considered the same, although they both have the same set of ϕ values. It seems that the structural order parameter q since it varies more strongly with the exact distances between amino acid pairs is a more demanding similarity measure than ϕ, which depends only on whether contacts form within a specified cutoff distance. Two residues that are closer than the cutoff distance for a contact but near that limit contribute strongly to ϕ, but lead to a low q_{ij} value for that residue pair, if the distance of the residue pair is very near in the reference transition state ensemble. Thus we see that using ϕ values alone for reconstruction may lead to discrepancies in short-ranged local structural elements such as the α-helical structures of the ensembles obtained with the replica simulation algorithm and the gold standard ensemble. Nevertheless both ϕ and q are adequate order parameters to quantify a conformation and its global fold.

Another question we can address is whether a larger λ parameter that would reflect the availability of more accurate data would eventually lead to precise reproduction of the reference ensemble. One might argue that increasing the strength of interaction, the λ parameter, could force the regenerated ensemble to approach the reference ensemble. KS tests have been performed with increasing value of λ, but they showed no noticeable improvement for the recovery of the reference ensemble with one replica. Apparently the structural imprecision of ϕ also plays a role in determining the fidelity of ensemble recovery. Without knowledge of the energy landscape of folding of the λ repressor, the KS test above indicates that one cannot conclude that the one-replica Hamiltonian will reliably deduce the reference ensemble even though it reproduces the set of experimental ϕ values. The reference ensemble is only partially reproduced using the one-replica simulation technique. Nevertheless, inversion with one replica can be judged to be partially successful.

In contrast to the one replica ensemble reproduction the curves of the overlap distributions for multiple replicas are bimodal. To check whether the bimodality of the replicas is an artifact of a recovered ensemble with unfolded and folded structures, that on average match the reference ϕ values, the probability distribution of the recovered ensemble obtained with the eight replica algorithm is plotted. The average ϕ value of each snapshot is calculated and the results are binned in bins of size of 0.005. The reference ensemble is
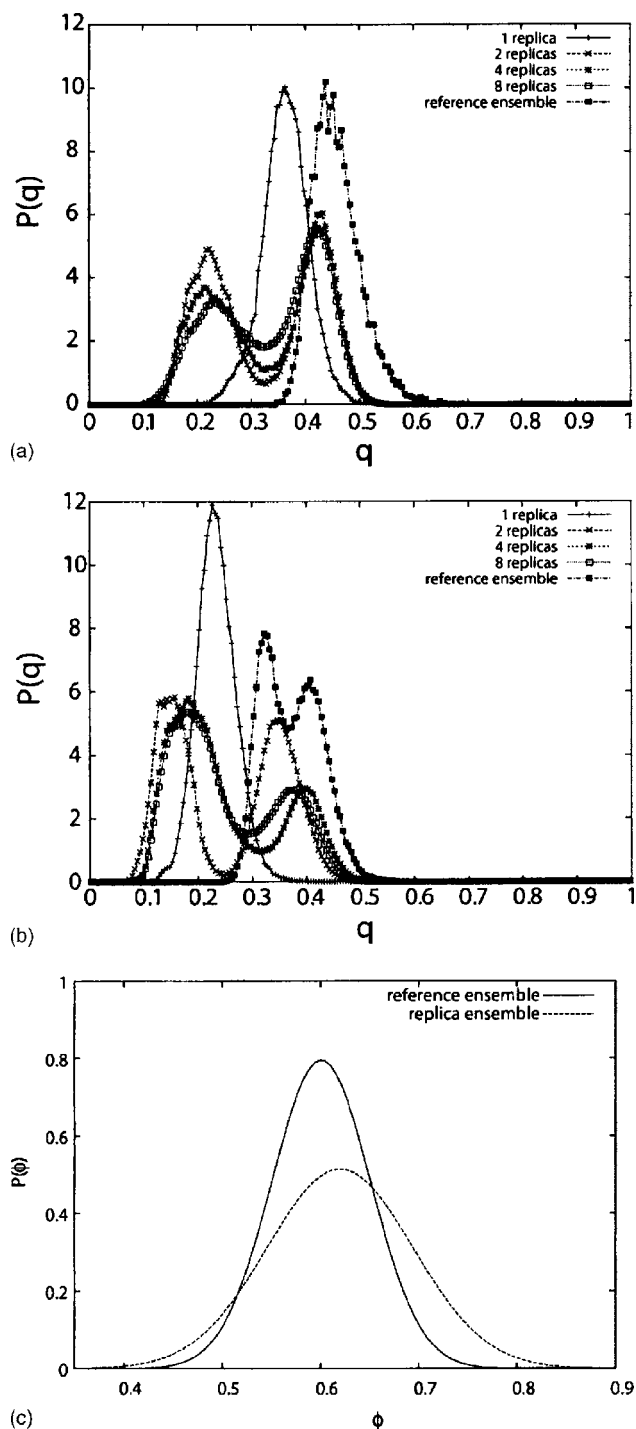

FIG. 3. Shown are the overlap distributions at the folding temperature of the ensembles obtained from replica simulations with the reference ensemble, for the three different transition state ensembles with $p=1$ (a) and $p=3$ (b). The self-overlap distribution of the reference ensemble is also shown. In the one replica case the distribution of overlaps with the reference ensemble is different from the reference self-overlap distribution, indicating the two ensembles are different although the ϕ values were recovered with the one-replica Hamiltonian. Increasing the parameter λ (not shown) did not result in better reproduction of the ensemble. The overlap distribution functions of the multiple-replica ensembles with the reference ensemble show bimodal distributions with one part of the distribution overlapping well with the self-overlap distribution of the reference ensemble. To assure that the bimodality of the probability distribution of the recovered ensembles stems from a nontrivial replica symmetry breaking, rather than the trivial case of merging ensembles of completely folded and unfolded replicas, the probability distribution of the average ϕ value of each individual realization in the recovered ensemble with eight replicas is plotted in (c).
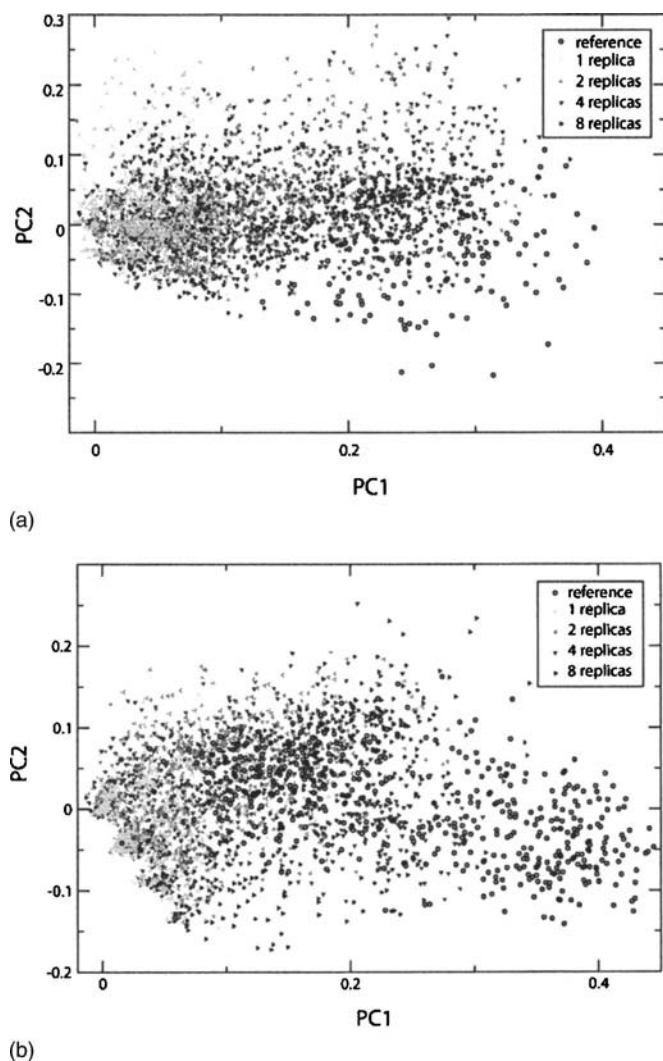
(a)

(b)

FIG. 4. The two principal components of conformations found in the reference ensemble and ensembles obtained with the replica algorithm with one to eight copies for the $p=1$ case (a) and the $p=3$ case (b) are shown.
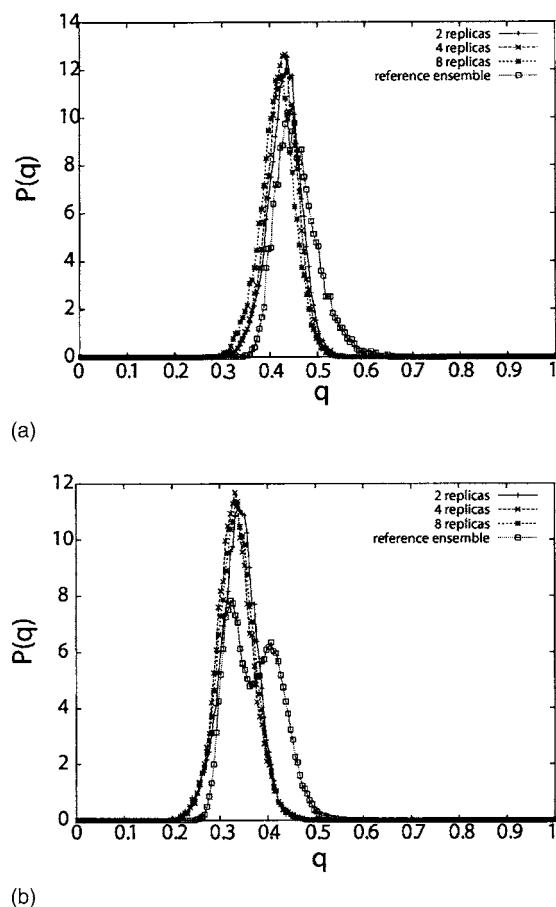

(a)

(b)

FIG. 5. Overlap distributions of the reduced ensembles from the replica simulations for 2, 4, and 8 replicas with the $p=1$ (a) and the $p=3$ (b) ensemble. The ensembles obtained from the clustering technique described in the method section improved the prediction success of the experimental ensemble for $p=1$ tremendously as measured by the KS test. For the $p=3$ ensemble the reduced ensembles reproduce the reference ensemble as measured by the KS test partially.

also plotted for comparison. One of the two peaks of the overlap distribution overlaps well with the reference ensemble probability distribution suggesting that the ensembles are similar. These results suggest that the reference ensemble can be extracted from the ensemble obtained with simulations with multiple replicas. The nature of the bimodal probability distribution suggests that the replicas are not homogeneous but instead break the replica symmetry. It is clear from Fig. 3(c) that the broken replica symmetry does not stem from a simple division of folded and unfolded structures of the recovered ensemble. The underlying replica symmetry breaking is more subtle. The distribution of the average ϕ value of each realization (or snapshot) of the recovered ensemble is similar to the distribution of average ϕ values of the reference ensemble.

IV. SAMPLING ENHANCEMENT THROUGH MULTIPLE REPLICAS

Principal component analysis of the contact maps of each structure allows a convenient visualization of the patterns of variation in contact probabilities in the subensembles

and hence allows the study of the range of conformations of all residues in those structural ensembles. Figure 4 displays the conformations of the structures of the reference ensemble and the regenerated ensembles for one to eight replicas projected onto the first two principal components. In the $p=1$ case the first principal component is a good indication of the sampling of the reference ensemble. The reference ensemble shows a negative first principal component (PC1) with most conformations in the region of PC $1=-2$ to -4. The projections of the conformations obtained with multiple replicas show much more overlap with the reference ensemble than the projections of the one replica conformations. The recreated ensemble obtained with multiple replicas is substantially shifted towards more negative PC1 when compared to the one replica ensemble. The multiple replica algorithm better samples reference-ensemble-like structures than does the single replica algorithm although the number of independent samples is kept equal between all replica simulation runs of single and multiple copies. To test whether the degree of overlap of each of the multiple replica ensembles with the reference ensemble is artificially high due to the fact that all ensembles including the single replica ensemble enter the PCA, analysis of the individual multiple replica ensembles
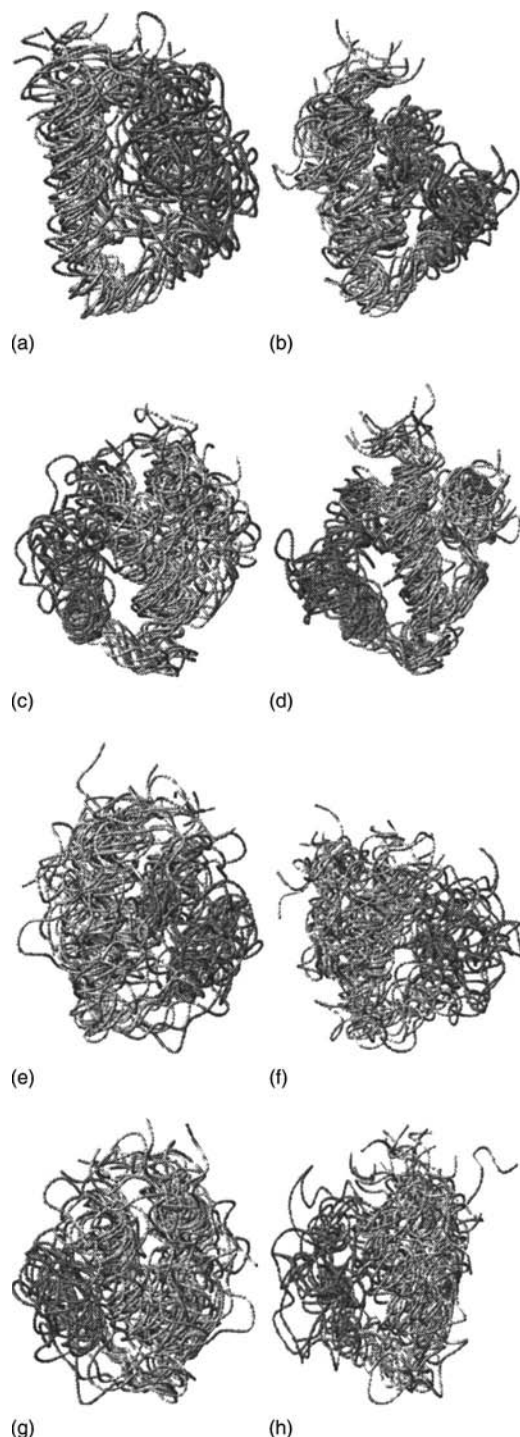
FIG. 6. Shown are the reference transition state ensembles viewed from front [(a) and (e)] and back [(c) and (g)] and the reduced ensembles obtained with eight replicas for $p=1$ and 3. The DNA binding region (green) is disordered in the transition state. For the $p=1$ case the reduced ensemble [(b) and (d)] and the reference ensemble [(a) and (c)] show the same intrinsic features such as secondary and tertiary structures and their average structure has a relative RMSD of the backbone carbons of less than 2.5 Å. For the $p=3$ case both of the reduced ensemble overlayed [(f) and (h)] show similar structural features than the reference ensemble [(e) and (g)]. Pictures were made with MOLMOL (Ref. 27).

with the reference ensemble has been performed, which shows very similar results. The advantage of the multiple replica algorithm seems even more apparent for the $p=3$ reference ensemble. Here the reference ensemble is bimodal

as reflected in the results of the principal component analysis [Fig. 4(b)]. The reference ensemble structures projected onto the principal components show two main clusters. While the ensemble obtained with one replica shows only small overlap with the reference ensemble located in the PC1 region of less than 2, there is no overlap with the reference ensemble conformations projected along the PC1 greater than 2. The PC1 of the ensembles obtained with multiple replicas assume a wider range of PC1 values indicating the better sampling of both clusters of reference ensemble structures. The success of multiple replicas is due to the fact that multiplicity of replicas allows fluctuations around the ϕ values for individual structures, while still constraining the replicas on average to its input ϕ values. We also projected the first two principal components onto the contact map of the λ repressor (data not shown). The contact maps are convenient to visualize on a residue-residue contact basis, which residues are more reference-ensemble-like and which are not. Most contacts that are formed in the reference ensemble are also formed equally in the replica ensembles. Structurally, the main differences between the reference and the replica ensembles can be contributed to the different C-terminal helix contacts.

V. REFERENCE ENSEMBLE RECREATION THROUGH ENSEMBLE REDUCTION METHODS

A powerful adjunct for the recreation procedure would be to have some kind of selection filter for the structures obtained in a simulation. If a postprocessing tool were to exist that allowed the selection of only those structures that truly resemble the reference ensemble, the somehow usefulness of the inversion procedure would be greatly enhanced. There are many possible ways of partitioning the ensemble based on the structural diversity. A simple clustering algorithm that clusters structures obtained with the multiple-replica Hamiltonian allows separation of these structures into subensembles. The Fitch-Margoliash clustering algorithm uses a distance measure between all structures to generate a phylogenetic tree. The distance parameter d is given by $d=1-q$, where q is a normalized pairwise measure of similarity of all structures relative to each other. For the $p=1$ transition state ensemble the phylogenetic tree showed clustering into two main clusters. One cluster contained structures with greater variation of the radius of gyration and less helical content. This cluster was not as homogeneous as the other cluster was. It contained lots of subclusters. The other cluster showed more compact structures with higher helical content. The structures of this cluster are denoted the "reduced ensemble." It was then confirmed that this ensemble has on average the same set of ϕ values as the reference ensemble. This is important in validating the choice of the most dominant subensemble as a valid representation of the reference ensemble. If the difference between the average ϕ values of the reference ensemble and the chosen cluster are large, the cluster cannot be accepted as a valid ensemble. However, there was no such difficulty for the most dominant cluster. KS tests with the reduced ensembles were performed to test
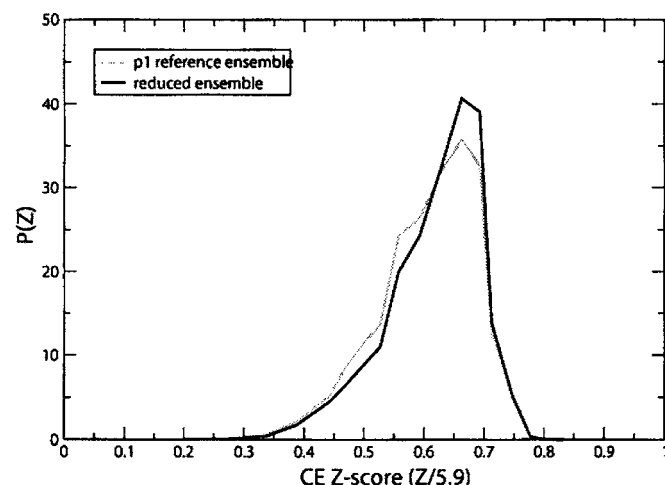
(a)
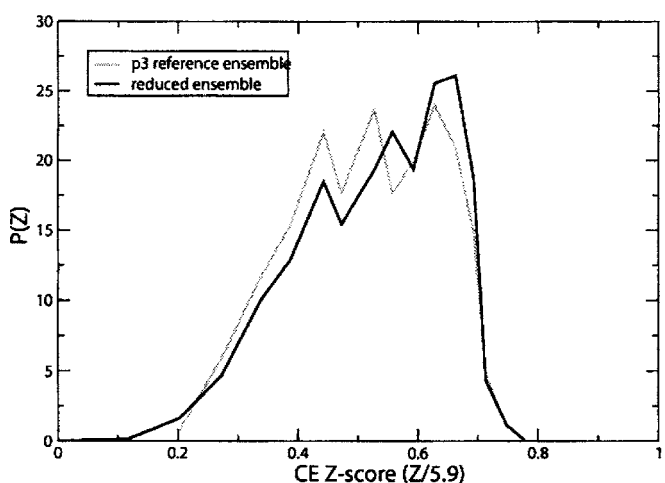
(b)

FIG. 7. KS overlap test of the reduced ensemble obtained with eight replicas and their corresponding reference ensemble using the CE Z score as reaction coordinate for the $p=1$ (a) and $p=3$ (b) ensemble.

whether these ensembles overlapped with the $p=1$ reference ensemble. The overlap of the reduced ensemble for multiple replicas with the experimental $p=1$ reference ensemble suggested a successful recovery of the reference transition state ensemble [Fig. 5(a)]. The structures of the reduced ensemble [Figs. 6(b) and 6(d)] exhibited the same global fold with similar disorder in the DNA binding region as the reference ensemble [Figs. 6(a) and 6(c)]. All structural comparisons such as root mean square deviation (RMSD), helical content, radius of gyration, secondary and tertiary structures, and Z score from the combinatorial extensions algorithm (the CE Z score) confirmed that these two ensembles are indeed equivalent on the basis of each of these measures. The phylogenetic tree was also obtained for structures obtained with the multiple-replica algorithm for the $p=3$ case. The tree showed a main cluster with a few populated subclusters. The structures of the subcluster whose average ϕ-values resemble the most the reference ensemble were taken as the reduced ensemble. The KS test was then performed for the reduced ensemble. The result is shown in Fig. 5(b). The probability distribution function of q overlap of the $p=3$ reference tran-

sition state ensemble shows a bimodal distribution. The probability distribution of the reduced ensembles overlapped well with one peak of the $p=3$ reference ensemble probability distribution. The structures found in the lower-q peak of the reference ensemble were compared to the structures of the reduced ensemble. The resultant structures of the replica simulations [Figs. 6(f) and 6(h)] exhibit similar tertiary and secondary structures to that of reference ensemble structures [Figs. 6(e) and 6(g)]. Using other order parameters in the KS test, such as the CE Z score or RMSD, supports the results of the KS test that the reduced ensemble and the lower-q reference ensemble are highly similar ensembles. In Figs. 7(a) and 7(b) we show the overlap distributions of the reduced ensemble obtained with eight replicas and their corresponding reference ensemble. We note that the CE Z score is downscaled by a factor of 5.9, which is the resulting score for the overlap of each of the transition state structures to themselves. This will normalize the CE Z-score axis to facilitate better comparison to the order parameter Q. The $p=1$ reference ensemble distribution peaks at a Z score of about $0.67 \times 5.9 = 3.95$ and most structures have a Z score in the range of 3.65–4.19. A Z score of 3.5 and higher is considered a criterion that the two structures share the same fold. We therefore see that in the $p=1$ reference transition state ensemble structures and folds are very similar to each other. The KS test using the CE Z score as a reaction coordinate shows the high overlap of the probability distributions of the reduced ensemble and the reference ensemble. The conclusion from the Z-score overlap test is that the two ensembles, reference and reduced ensembles, are indeed equivalent ensembles in terms of representing the same distribution of global folds. The $p=3$ reference ensemble showed a bimodal distribution in the order parameter q with larger variations of relative structural similarity. As one would expect, nonadditivity causes the folds in this transition state ensemble to be less homogeneous than those in the $p=1$ reference ensemble. Indeed a wider range of CE Z scores of $\sim$2.36–4.10 is found within the reference ensemble itself. The overlap between the lower q subensemble of the $p=3$ reference ensemble and the reduced ensemble is excellent indicating that the folds in the reference subensemble are well represented in the reduced ensemble and that ensemble recovery judged by CE Z score and the KS test has been very successful for these reference structures. The CE Z score is traditionally used for fold recognition. The probability distribution of the overlap function shows that the reduced ensemble does have the same distribution of global folds than the reference ensemble, which is not surprising since the average ϕ values are reproduced. For the order parameter q, the dominant subensemble obtained by the clustering method only represents part (although most) of the $p=3$ reference transition state ensemble. Without knowledge of the energy landscape of the protein, the reduction method cannot be used to completely reproduce the reference ensembles. If further low resolution experiments are known, additional clusters can be identified that resemble the real gold standard ensemble.

VI. ROBUSTNESS OF THE PREDICTION OF THE TRANSITON STATE ENSEMBLE FOR THE λ REPRESSOR

To test the robustness of the ability of replica simulations to recover reference ensembles from imperfect laboratory experiments, we introduced perturbations in the input data resembling experimental errors. To obtain these results we therefore stochastically changed the set of ϕ values used in the reconstruction to see whether an ensemble could nevertheless be recreated that was faithful to the gold standard ensemble. To do this first a new set of ϕ values was created by randomly picking a ϕ value for each residue from a Gaussian distribution, having a mean value corresponding to the gold standard ϕ value with a standard deviation given by the experimentally expected standard deviation of the measurement of that ϕ value. The magnitude of the errors introduced was of the order of 20% for the $p=1$ reference ensemble ϕ values and about 30% for the $p=3$ reference ensemble. These new perturbed lists of ϕ values then served as an experimental input for the replica Hamiltonian. Replica simulations with these new ϕ values were performed and the resulting transition state ensembles were compared to the reference ensemble with the KS overlap test. In the case of the $p=1$ transition state ensemble, the overlap distribution of the ensemble obtained with one replica using the new noisy ϕ values no longer coincides with the distribution of overlaps within the gold standard reference ensemble at all [Fig. 8(a)]. The overlap distributions show that the two ensembles are rather different. Simulations using a single replica appear rather sensitive towards uncertainties in ϕ and fail to result in successful ensemble recreation.

In contrast, the overlap distributions for ensembles obtained with multiple replicas do show considerable overlap with the distribution of the reference ensemble even when errors are introduced [Fig. 8(a)] at least in the $p=1$ case. The replicas are able to compensate the uncertainties in ϕ and partially reproduce the reference ensemble. It is also found that clustering of structures with the Fitch-Margoliash clustering algorithm yields at least one cluster with secondary and tertiary structures comparable to the reference transition state ensemble. The multiple-replica ensemble algorithm combined with selection through structural clustering therefore does successfully reproduce the $p=1$ reference ensemble. However, the structures obtained in replica simulations, that should reflect the reference ensemble of the $p=3$ transition state ensemble, are structurally different from those in the reference ensemble. The KS test shows that in no case can the replica simulation algorithm recreate the actual reference ensemble structures [Fig. 8(b)]. The $p=3$ transition state ensemble was obtained with a Hamiltonian, that leads to highly cooperative behavior. The folding under this Hamiltonian should resemble the folding of a protein that folds by forming a specific, determined folding nucleus. The ϕ values in the transition state ensemble are then expected to be less uniformly distributed with certain core residues being formed much earlier than the rest of the contacts. The errors introduced in ϕ are large and can potentially smear out the ϕ values resulting in a mean-field-like set of ϕ values, which are more uniformly distributed like the ϕ values of the p
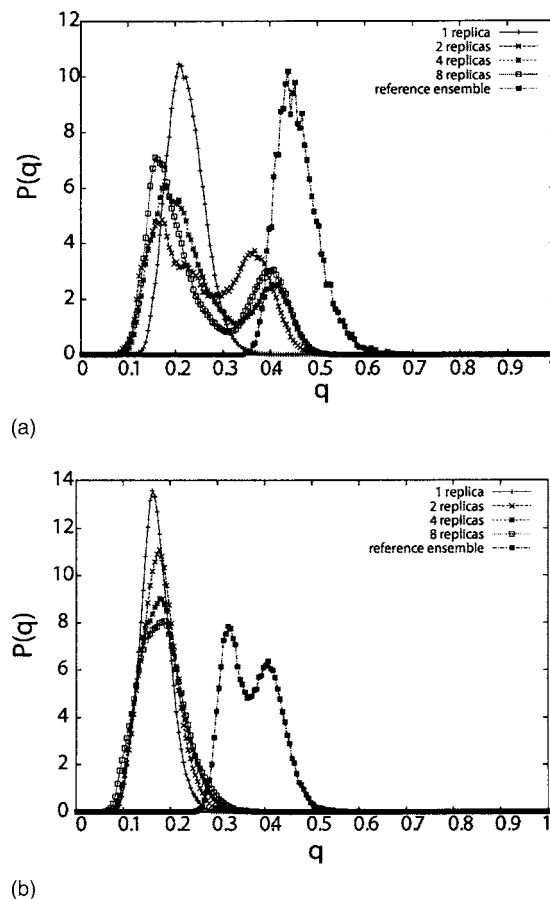

(a)

(b)

FIG. 8. Overlap distributions for the $p=1$ and $p=3$ transition state ensemble for 1, 2, 4, and 8 replicas. For $p=3$ the new set of ϕ values generated structures, that did not overlap with the reference ensemble at all. In the $p=1$ case the overlap was smaller when compared to the overlap in Fig. 3.

$=1$ transition state ensemble. This effect of creating a more uniform set of ϕ values could be a possible explanation, why recreating the transition state ensemble of the λ repressor obtained with a very nonadditive Hamiltonian is more sensitive to errors in ϕ than is the recreation for the $p=1$ ensemble.

VII. CONCLUSION

Scientists often seek to invert hard won experimental data with the hope to obtain statistically correct structural ensembles with high fidelity. We see that the ability of successfully doing this for structural ensembles of partially folded biomolecules depends on the algorithm employed and on the quality of the measured data we seek to recreate.

First consider the $p=1$ reference ensemble. This ensemble has a unimodal overlap distribution and corresponds to a low transition state barrier with structures that are close in Q being close in free energy. Our simulation results with the molecular dynamics replica algorithm show that this algorithm can partially recreate the correct reference transition state ensembles from the set of ensemble-averaged ϕ values. For the $p=1$ reference ensemble, structures obtained in simulations with one replica show overlap in the $P(q)$ distribution with the reference ensemble. The KS test shows, however, that the distributions of the reference ensemble and the en-

semble obtained from the replica algorithm are not the same despite the fact that the ensembles share the same set of ϕ values. The one-replica algorithm partially reproduces the reference ensemble, that has a unimodal $P(q)$ distribution with large errors in ϕ and few non-native contacts. On the other hand, the ensembles obtained with multiple replicas show a bimodal distribution in the probability distribution of overlap with the reference ensemble with only one peak strongly overlapping with the reference ensemble. The rather small overlap suggests that structural clustering could yield a small cluster of structures, that would better resemble the reference ensemble. Clustering of the structures with the Fitch-Margoliash algorithm shows two main basins of structures. A reduced ensemble obtained from this clustering analysis reproduces the reference ensemble as measured by the KS test. These results suggest that when a single replica suffices to reproduce the reference ensemble, ensemble recreation with multiple replicas does so too.

We also examined how stable the inversion is when errors mimicking those found in experimental determinations are introduced. This study shows an additional advantage of introducing multiple replicas. Whereas the one-replica algorithm could not recreate the reference ensembles [Fig. 8(a)] at all from error ridden input, the multiple-replica algorithm combined with structural clustering analysis is able to produce a reduced ensemble that has the same structural characteristics as the reference ensemble. Ensembles with low free energy barrier, from which a set of ϕ values with large experimental errors is deduced, can only be inverted when multiple replicas coupled with structural clustering are introduced. For the $p=3$ transition state ensemble, the advantage of multiple replicas is also apparent. The ϕ values represent ensemble averaged quantities. The reference ensemble has a bimodal probability distribution as well as two clusters of conformations when observing these conformations projected onto the principal components. Each of these subensembles has also large fluctuations in their ϕ values. Hardly any individual structure in the reference transition state ensemble has the same set of ϕ values as the ensemble average set of ϕ values. In the inversion algorithm, the single replica algorithm recovers these individual structures. However, a successful recreation of the reference ensemble requires sampling of structures, that only on average reproduce the set of ϕ values. Introduction of multiple replicas allows fluctuations of microscopic ϕ's referring to these subensembles while the ϕ values averaged over all replicas still is constrained to its experimental value. The KS test and PCA show that multiple replicas do sample the dominant suben-

semble of the $p=3$ reference ensemble well. Few structures sampled the minority reference subensemble (the $PC1>2$ region, see Fig. 4), although the multiple replica algorithm does improve the ensemble recreation over the single replica case. Knowledge of the energy landscape of folding is only partially encoded in the ϕ values, thus adding additional *a priori* knowledge of the funneling of the energy landscape should help in inversion fidelity. Further work along these lines is planned.

[1] J. D. Bryngelson and P. G. Wolynes, Proc. Natl. Acad. Sci. U.S.A. **84**, 7524 (1987).
[2] C. Hardin, M. P. Eastwood, M. Prentiss, Z. Luthey-Schulten, and P. G. Wolynes, J. Comput. Chem. **23**, 138 (2002).
[3] J. N. Onuchic, Z. LutheySchulten, and P. G. Wolynes, Annu. Rev. Phys. Chem. **48**, 545 (1997).
[4] J. N. Onuchic, N. D. Socci, Z. LutheySchulten, and P. G. Wolynes, Folding Des. **1**, 441 (1996).
[5] A. Matouschek, J. T. Kellis, L. Serrano, and A. R. Fersht, Nature (London) **340**, 122 (1989).
[6] J. D. Bryngelson, J. N. Onuchic, N. D. Socci, and P. G. Wolynes, Proteins **21**, 167 (1995).
[7] E. Paci, M. Vendruscolo, C. M. Dobson, and M. Karplus, J. Mol. Biol. **324**, 151 (2002).
[8] K. Lindorff-Larsen, S. Kritjansdottir, K. Teilum, W. Fieber, C. M. Dobson, F. M. Poulsen, and M. Vendruscolo, J. Am. Chem. Soc. **126**, 3291 (2004).
[9] M. Vendruscolo and C. M. Dobson, Curr. Opin. Struct. Biol. **13**, 1 (2003).
[10] M. Vendruscolo, E. Paci, C. M. Dobson, and M. Karplus, Nature (London) **409**, 641 (2001).
[11] K. Lindorff-Larsen, M. Vendruscolo, E. Paci, and C. M. Dobson, Nat. Struct. Mol. Biol. **11**, 443 (2004).
[12] K. Lindorff-Larsen, R. B. Best, M. A. DePristo, C. M. Dobson, and M. Vendruscolo, Nature (London) **433**, 128 (2005).
[13] R. Davis, C. M. Dobson, and M. Vendruscolo, J. Chem. Phys. **117**, 9510 (2002).
[14] M. P. Eastwood and P. G. Wolynes, J. Chem. Phys. **114**, 4702 (2001).
[15] M. P. Eastwood, C. Hardin, Z. Luthey-Schulten, and P. G. Wolynes, J. Chem. Phys. **118**, 8500 (2003).
[16] N. Go, Annu. Rev. Biophys. Bioeng. **12**, 183 (1983).
[17] M. P. Eastwood, C. Hardin, Z. Luthey-Schulten, and P. G. Wolynes, IBM J. Res. Dev. **45**, 475 (2001).
[18] J. G. Saven and P. G. Wolynes, J. Mol. Biol. **257**, 199 (1996).
[19] J. N. Onuchic, N. D. Socci, Z. Luthey-Schulten, and P. G. Wolynes, Folding Des. **1**, 441 (1996).
[20] T. Shen, C. Zong, D. Hamelberg, J. A. McCammon, and P. G. Wolynes, FASEB J. **19**, 1389 (2005).
[21] W. M. Fitch and E. Margoliash, Science **155**, 279 (1967).
[22] J. Felsenstein, PHYLIP (Version 3.2), a phlylogeny inference package (1989), Cladistics 5: 164–166.
[23] G. S. Huang and T. G. Oas, Biochemistry **34**, 3884 (1995).
[24] L. J. Beamer and C. O. Pabo, J. Mol. Biol. **227**, 177 (1992).
[25] S. S. Cho, Y. Levy, and P. G. Wolynes, Proc. Natl. Acad. Sci. U.S.A. **103**, 586 (2006).
[26] M. R. Ejtehadi, S. P. Avall, and S. S. Plotkin, Proc. Natl. Acad. Sci. U.S.A. **101**, 15088 (2004).
[27] R. Koradi, M. Billeter, and K. Wuthrich, J. Mol. Graphics **14**, 51 (1996).